Mass Transport in Deep-Water Long-Crested Random Gravity Waves[1]

MING-SHUN CHANG

Department of Meteorology and Oceanography, New York University
New York, New York 10453

The theoretical and observed motions of a particle on the surface of deep-water long-crested random gravity waves are studied. The experiment was performed at the Stevens Institute of Technology. The theoretical model is formed in Lagrangian coordinates by applying perturbation and spectral techniques to the equations of motion for an incompressible fluid for both viscous and irrotational flows. The theoretical drift agrees very well with the observed mass transport. An important contribution consists of a large low-frequency oscillation about the mean drift that is correctly predicted by the second-order correction to the spectrum of the horizontal motion. Spectra, cross spectra, and bispectra are estimated from the data and all support the conclusions based on the irrotational model, which correctly describes the behavior of the particle.

INTRODUCTION

Stokes [1847] was the first to recognize that there is a steady second-order mean forward velocity of particles associated with gravity waves. He showed that, if the wave equation for the free surface elevation η is

$$\eta = ae^{i(kx-\omega t)} + O(a^2k)$$

where k is the wave number, a is the amplitude, and ω is the angular frequency, then the velocity of mass transport must be

$$\bar{U} = \frac{a^2\omega k \cosh 2k(z - h)}{2 \sinh^2 kh} + C$$

where h is the water depth and C is an arbitrary constant. If the total horizontal mass transport is assumed to be zero, one must have

$$C = -(a^2\omega/2h) \coth kh$$

In deep water, $kh \gg 1$, $\bar{U}$ simply becomes

$$\bar{U} = a^2\omega ke^{-2kz}$$

Laboratory experiments designed to measure the mass transport velocity have been performed by *de Caligny* [1878], the *Beach Erosion Board* [1941], *Bagnold* [1947], and *Longuet-Higgins* [1960]. All measurements suggested that Stokes' mass transport velocity equation is an unsatisfactory model. An observed strong forward velocity near the bottom and a backward velocity in between is not predicted by Stokes' model. The main reason for the discrepancy between observations and Stokes' model is the assumption of irrotationality. *Longuet-Higgins* [1953], carrying the analysis to the second order, found a markedly different result for a viscous fluid. In progressive waves, his mass transport velocity near the bottom was given by

$$\bar{U} = \frac{5}{4}\frac{a^2\omega k}{\sinh^2 kh}$$

and the velocity gradient near the surface was given by

$$\frac{\partial \bar{U}}{\partial z} = -4a^2\omega k \coth kh$$

This is twice the corresponding value of Stokes' model and compared quite well with tank measurements.

Ocean waves are not single sine waves; hence, neither Stokes' nor Longuet-Higgins' model can be applied to the real oceans. Therefore, another model is required that can apply to random waves. *Tick* [1959] derived a stationary random process with continuous spectrum that satisfied

[1] Contribution 72 of the Geophysical Sciences Laboratory, Department of Meteorology and Oceanography, New York University.

the perturbed equations of motion in Eulerian coordinates and obtained a nonlinear random model of gravity waves that tended to explain the second peak in the spectrum of gravity waves. *Pierson* [1961] solved the equations of motion in Lagrangian coordinates to second order for a nonviscous fluid and obtained an equivalent drift as determined by Stokes. In this paper, random process techniques are applied to the second-order perturbation equations of motion in Lagrangian coordinates for both the viscous and the nonviscous case.

Irrotational Flow

Governing equations. In meteorology and oceanography there are two basic ways to describe the motion of fluid particles, the Eulerian and Lagrangian representations. The Lagrangian representation will be considered here.

If X and Z (Z positive upward) represent the horizontal and vertical coordinates of a particle and α and δ represent the corresponding particle tags, or material coordinates, in the Lagrangian system, the inviscid two-dimensional equations of motion can be written as

$$X_{tt}X_\alpha + Z_{tt}Z_\alpha + gZ_\alpha + (P_\alpha/\rho) = 0 \quad (1)$$

$$X_{tt}X_\delta + Z_{tt}Z_\delta + gZ_\delta + (P_\delta/\rho) = 0 \quad (2)$$

where ρ is density, g is the acceleration of gravity, P is pressure, and the subscripts represent partial differentiation.

If the water is assumed to be incompressible, the Jacobian of these two coordinate systems can be set equal to unity; i.e.,

$$\partial(X, Z)/\partial(\alpha, \delta) = 1 \quad (3)$$

Also, if it is assumed that X, Z, and P can be expressed as a power series, then

$$X = \alpha + \epsilon x_1 + \epsilon^2 x_2 + \cdots$$
$$= \alpha + X_1 + X_2 + \cdots \quad (4)$$

$$Z = \delta + \epsilon z_1 + \epsilon^2 z_2 + \cdots$$
$$= \delta + Z_1 + Z_2 + \cdots \quad (5)$$

$$P = -\rho g\delta + \epsilon p_1 + \epsilon^2 p_2 + \cdots$$
$$= -\rho g\delta + P_1 + P_2 + \cdots \quad (6)$$

where ϵ is a small quantity. These equations with $\epsilon = 0$ correspond to the unperturbed system at rest.

After substituting (4), (5), and (6) into (1), (2), and (3) and equating the coefficients of ϵ and ϵ^2, one obtains

ϵ equations

$$X_{1tt} + gZ_{1\alpha} + (P_{1\alpha}/\rho) = 0 \quad (7)$$

$$Z_{1tt} + gZ_{1\delta} + (P_{1\delta}/\rho) = 0 \quad (8)$$

$$X_{1\alpha} + Z_{1\delta} = 0 \quad (9)$$

ϵ^2 equations

$$X_{2tt} + gZ_{2\alpha} + (P_{2\alpha}/\rho) + X_{1\alpha}X_{1tt} + Z_{1\alpha}Z_{1tt} = 0 \quad (10)$$

$$Z_{2tt} + gZ_{2\delta} + (P_{2\delta}/\rho) + X_{1\delta}X_{1tt} + Z_{1\delta}Z_{1tt} = 0 \quad (11)$$

$$X_{2\alpha} + Z_{2\delta} + Z_{1\delta}X_{1\alpha} - X_{1\delta}Z_{1\alpha} = 0 \quad (12)$$

Expressions for X_1, X_2, Z_1, Z_2, P_1, and P_2 can then be obtained from the two sets of equations above by imposing suitable boundary conditions. If an infinitely deep body of water with a free upper surface and an unlimited fetch is considered, the boundary conditions are that $P_1 = P_2 = 0$ at the free surface ($\delta = 0$) and that P_1, P_2, Z_1, and Z_2 become zero as $\delta \to -\infty$.

First-order solution. Eliminating P_1 from (7) and (8), one obtains

$$X_{1\delta tt} - Z_{1\alpha tt} = 0 \quad (13)$$

With (9) one has the differential equations (14 and 15) for X_1 and Z_1

$$X_{1\alpha\alpha tt} + X_{1\delta\delta tt} = 0 \quad (14)$$

$$Z_{1\alpha\alpha tt} + Z_{1\delta\delta tt} = 0 \quad (15)$$

Under the assumption that X, Z, and P are stationary random processes with respect to α and t, the spectral representations are

$$X = \iint_{-\infty}^{\infty} e^{i(k\alpha - \omega t)} \cdot d\xi'_{(x)}(k, \omega; \delta) + M_{(x)} \quad (16)$$

$$Z = \iint_{-\infty}^{\infty} e^{i(k\alpha - \omega t)} \cdot d\xi'_{(z)}(k, \omega; \delta) + M_{(z)} \quad (17)$$

$$P = \iint_{-\infty}^{\infty} e^{i(k\alpha - \omega t)} \cdot d\xi'_{(p)}(k, \omega; \delta) + M_{(p)} \quad (18)$$

where the expected value of $d\xi'$ is given as

$$E[d\xi'(k, \omega; \delta)\ \overline{d\xi'(k', \omega'; \delta)}] = \begin{cases} dS(k, \omega; \delta) & \text{if } k = k', \quad \omega = \omega' \\ 0 & \text{otherwise} \end{cases}$$

The overbar denotes the complex conjugate.

In the above expression $S(k, \omega; \delta)$ is the spectral distribution function and M is the mean that is assumed to be the unperturbed value.

Since X_1, Z_1 satisfy (14) and (15), one obtains

$$X_1 = \iint_{-\infty}^{\infty} e^{i(k\alpha - \omega t)} e^{|k|\delta}\ d\xi_{1(x)}(k, \omega) + \iint_{-\infty}^{\infty} e^{i(k\alpha - \omega t)} e^{-|k|\delta}\ d\xi''_{1(x)}\ (k, \omega) \quad (19)$$

$$Z_1 = \iint_{-\infty}^{\infty} e^{i(k\alpha - \omega t)} e^{|k|\delta}\ d\xi_{1(z)}(k, \omega) + \iint_{-\infty}^{\infty} e^{i(k\alpha - \omega t)} e^{-|k|\delta}\ d\xi''_{1(z)}\ (k, \omega) \quad (20)$$

For deep water the second term on the right-hand sides of (19) and (20) must vanish owing to the boundary condition as the depth becomes infinite. Hence, X_1 and Z_1 simply become

$$X_1 = \iint_{-\infty}^{\infty} e^{i(k\alpha - \omega t)} e^{|k|\delta}\ d\xi_{1(x)}(k, \omega) \quad (21)$$

$$Z_1 = \iint_{-\infty}^{\infty} e^{i(k\alpha - \omega t)} e^{|k|\delta}\ d\xi_{1(z)}(k, \omega) \quad (22)$$

Substituting (21) and (22) into (13), one obtains

$$\iint_{-\infty}^{\infty} ike^{i(k\alpha - \omega t)} e^{|k|\delta}\ d\xi_{1(x)}(k, \omega) + \iint_{-\infty}^{\infty} |k|\ e^{i(k\alpha - \omega t)} e^{|k|\delta}\ d\xi_{1(z)}(k, \omega) \equiv 0 \quad (23)$$

To satisfy the above identity, it is required that

$$ik\ d\xi_{1(x)}(k, \omega) + |k|\ d\xi_{1(z)}(k, \omega) = 0$$

Since $d\xi_{1(x)}(k, \omega) \equiv d\xi_{1(z)}(k, \omega) \equiv 0$ is a trivial solution, it follows that

$$d\xi_{1(z)}(k, \omega) = -i \frac{k}{|k|}\ d\xi_{1(x)}(k, \omega) \quad (24)$$

Hence, the solution of Z_1 becomes

$$Z_1 = \iint_{-\infty}^{\infty} - i \frac{k}{|k|} \cdot e^{i(k\alpha - \omega t)} e^{|k|\delta}\ d\xi_{1(x)}(k, \omega) \quad (25)$$

From the boundary condition at the free surface of the irrotational flow, $P_1 = 0$, at $\delta = 0$, one obtains

$$\iint_{-\infty}^{\infty} \left[-\omega^2 + (ikg)\left(-i \frac{k}{|k|} \right) \right] \cdot e^{i(k\alpha - \omega t)}\ d\xi_{1(x)}(k, \omega) = 0 \quad (26)$$

Also, the condition that $d\xi_{1(x)}(k, \omega)$ is not zero requires that

$$k = |\omega|\ \omega/g \quad (27)$$

in order to satisfy (26).

The spectral representations of X_1, Z_1, and P_1 have now been reduced to one-dimensional random processes and are expressed as

$$X_1 = \int_{-\infty}^{\infty} e^{i[(|\omega|\omega/g)\alpha - \omega t]} \cdot e^{(\omega^2/g)\delta}\ d\xi_{1(x)}(\omega) \quad (28)$$

$$Z_1 = \int_{-\infty}^{\infty} -i \frac{\omega}{|\omega|} \cdot e^{i[(|\omega|\omega/g)\alpha - \omega t]} e^{(\omega^2/g)\delta}\ d\xi_{1(x)}(\omega) \quad (29)$$

$$P_1 = 0 \quad (30)$$

Second-order solution. The second-order solutions can be obtained from substitution of (28), (29), and (30) into (10), (11), and (12), respectively. These substitutions yield

$$X_{2tt} + gZ_{2\alpha} + P_{2\alpha}/\rho = 0 \quad (31)$$

$$Z_{2tt} + gZ_{2\delta} + P_{2\delta}/\rho = \iint_{-\infty}^{\infty} \omega^2 \left[\frac{\omega'^2}{g} - \frac{\omega'^2}{g} \operatorname{sgn}(\omega\omega') \right] \cdot e^{i[(\omega^{*2}/g)\alpha - (\omega + \omega')t]} \cdot e^{[(\omega^2/g) + (\omega'^2/g)]\delta}\ d\xi_{1(x)}(\omega)\ d\xi_{1(x)}(\omega') \quad (32)$$

$$X_{2\alpha} + Z_{2\delta} = \iint_{-\infty}^{\infty} \left[\frac{\omega^2\omega'^2}{g^2} - \frac{\omega^2\omega'^2}{g^2} \operatorname{sgn}(\omega\omega') \right] \cdot e^{i[(\omega^{*2}/g)\alpha - (\omega + \omega')t]} \cdot e^{[(\omega^2/g) + (\omega'^2/g)\delta]}\ d\xi_{1(x)}(\omega)\ d\xi_{1(x)}(\omega') \quad (33)$$

where $\omega^{*2} = |\omega|\omega + |\omega'|\omega'$.

The homogeneous solutions of the above set of equations are clearly

$$X_2^* = \iint_{-\infty}^{\infty} e^{i[(\omega^{*2}/g)\alpha-(\omega+\omega')t]} \cdot e^{|\omega^{*2}/g|\delta}\, d\xi_{2(x)}^*(\omega, \omega') \quad (34)$$

$$Z_2^* = \iint_{-\infty}^{\infty} -i \operatorname{sgn}(\omega+\omega') \cdot e^{i[(\omega^{*2}/g)\alpha-(\omega+\omega')t]} e^{|\omega^{*2}/g|\delta}\, d\xi_{2(x)}^*(\omega, \omega') \quad (35)$$

$$P_2^* = \iint_{-\infty}^{\infty} -i\rho g B e^{i[(\omega^{*2}/g)\alpha-(\omega+\omega')t]} \cdot e^{|\omega^{*2}/g|\delta}\, d\xi_{2(x)}^*(\omega, \omega') \quad (36)$$

where

$$B = [(\omega+\omega')^2 - |\omega^{*2}|]/\omega^{*2} \quad (37)$$

To obtain the inhomogeneous solutions, the integrations on the right-hand sides of (31), (32), and (33) are separated into three parts: over the plane $\omega\omega' \geq 0$, the neighborhood of line $\omega = -\omega$, and the remaining portion (R) of the $\omega\omega'$ plane. The contribution to the inhomogeneous solutions from the first part of the integration is equal to zero. The inhomogeneous solution contributed by the second part of the integral is obtained by the method of elimination of variables, and it is written

$$Z_2^{**} = \int_0^{\infty} \frac{2\omega^2}{g} e^{(2\omega^2/g)\delta}\, d\xi_{1(x)}(\omega)\, d\xi_{1(x)}(-\omega) \quad (38)$$

$$X_2^{**} = \int_{-\infty}^{\infty} A(\delta, t, \omega)\, d\xi_{1(x)}(\omega)\, d\xi_{1(x)}(-\omega) \quad (39)$$

$$P_2^{**} = 0$$

The integral over the region R has the same form as (31), (32), and (33). The inhomogeneous solutions to this integral are obtained by repeating the same procedures used to solve the first-order equations. The resulting expressions are

$$X_2^{***} = i \iint_R C e^{i[(\omega^{*2}/g)\alpha-(\omega+\omega')t]} \cdot e^{[(\omega^2/g)+(\omega'^2/g)]\delta}\, d\xi_{1(x)}(\omega)\, d\xi_{1(x)}(\omega') \quad (40)$$

$$Z_2^{***} = \iint_R D e^{i[(\omega^{*2}/g)\alpha-(\omega+\omega')t]} \cdot e^{[(\omega^2/g)+(\omega'^2/g)]\delta}\, d\xi_{1(x)}(\omega)\, d\xi_{1(x)}(\omega') \quad (41)$$

$$P_2^{***} = \iint_R \rho g E e^{i[(\omega^{*2}/g)\alpha-(\omega+\omega')t]} \cdot e^{[(\omega^2/g)+(\omega'^2/g)]}\, d\xi_{1(x)}(\omega)\, d\xi_{1(x)}(\omega') \quad (42)$$

where

$$C = \frac{1}{g} \frac{|\omega^3| + |\omega'^3|}{(\omega+\omega')} \quad (43)$$

$$D = \frac{\omega^2 - \omega\omega' + \omega'^2}{g} \quad (44)$$

$$E = \frac{C(\omega+\omega')^2 - D(\omega^{*2})}{\omega^{*2}} \quad (45)$$

Since the general solution is the sum of the homogeneous and inhomogeneous solutions, it is written as

$$X_2 = X_2^* + X_2^{**} + X_2^{***} \quad (46)$$

$$Z_2 = Z_2^* + Z_2^{**} + Z_2^{***} \quad (47)$$

$$P_2 = P_2^* + P_2^{***} \quad (48)$$

where these quantities are the same as defined above.

From the boundary condition at the free surface ($P_2 = P_2^* + P_2^{***} = 0$), the function $d\xi_{2(x)}^*(\omega, \omega')$ can be defined as

$$d\xi_{2(x)}^*(\omega\ \omega') = \begin{cases} -iM = -i\dfrac{E}{B}\, d\xi_{1(x)}(\omega)\, d\xi_{1(x)}(\omega') & \text{over } R \\ 0 & \text{otherwise} \end{cases} \quad (49)$$

If the motion of the fluid is started from rest, then under the irrotational assumption, the vorticity of the fluid is always equal to zero. Therefore, there must exist a function, say, $F(\alpha, \delta, t)$ such that

$$dF = (X_t X_\alpha + Z_t Z_\alpha)\, d\alpha + (X_t X_\delta + Z_t Z_\delta)\, d\delta \quad (50)$$

is a perfect differential. Linearizing the above equations, one obtains

$$dF_1 = X_{1t}\, d\alpha + Z_{1t}\, d\delta \quad (51)$$

$$dF_2 = (X_{2t} + X_{1t}X_{1\alpha} + Z_{1t}Z_{1\alpha})\, d\alpha + (Z_{2t} + X_{1t}X_{1\delta} + Z_{1t}Z_{1\delta})\, d\delta \quad (52)$$

On substituting (28), (29), (46), (47), and (49) into (51) and (52), one obtains

$$dF_1 = -i\left[\int_{-\infty}^{\infty} \omega e^{i[(|\omega|\omega/g)\alpha - \omega t]} \cdot e^{(\omega^2/g)\delta}\, d\xi_{1(x)}(\omega)\right] d\alpha - \left[\int_{-\infty}^{\infty} |\omega|\, e^{i[(|\omega|\omega/g)\alpha - \omega t)]} \cdot e^{(\omega^2/g)\delta}\, d\xi_{1(x)}(\omega)\right] d\delta \quad (53)$$

$$dF_2 = \left[\iint_{-\infty}^{\infty} (I(\omega, \omega')e^{|\omega^{*2}/g|\delta} + G(\omega, \omega')e^{[(\omega^2/g)+(\omega'^2/g)]\delta}) \cdot e^{i[(\omega^{*2}/g)\alpha - (\omega+\omega')t]}\, d\xi_{1(x)}(\omega)\, d\xi_{1(x)}(\omega')\right] d\alpha + \left[\iint_{-\infty}^{\infty} (N(\omega, \omega')e^{|\omega^{*2}/g|\delta} + Q(\omega, \omega')e^{[(\omega^2/g)+(\omega'^2/g)]\delta}) \cdot e^{i[(\omega^{*2}/g)\alpha - (\omega+\omega')t]}\, d\xi_{1(x)}(\omega)\, d\xi_{1(x)}(\omega')\right] d\delta \quad (54)$$

where

$$I(\omega, \omega') = \begin{cases} \dfrac{-\omega^{**}(\omega^2 - \omega'^2)}{g} & \text{if } \omega\omega' < 0 \text{ and } \omega > 0 \\ \dfrac{\omega^{**}(\omega^2 - \omega'^2)}{g} & \text{if } \omega\omega' < 0 \text{ and } \omega < 0 \\ 0 & \text{otherwise} \end{cases}$$

$$G(\omega, \omega') = \begin{cases} \dfrac{1}{g}[(|\omega^3| + |\omega'^3|) + \omega'\omega(|\omega| + |\omega'|)] & \text{over } R \\ \dfrac{1}{g}[\omega\omega'(|\omega| + |\omega'|)] + A_t & \text{on the line } -\omega = \omega' \\ 0 & \text{otherwise} \end{cases}$$

$$N = \begin{cases} \dfrac{i}{g}\omega^{**}(|\omega^2 - \omega'^2|) & \text{over } R \\ 0 & \text{otherwise} \end{cases}$$

$$Q = \begin{cases} -i(\omega^3 + \omega^2\omega' + \omega\omega'^2 + \omega'^3) & \text{over } R \\ 0 & \text{otherwise} \end{cases}$$

$$\omega^{**} = \begin{cases} \omega & \text{if } |\omega| > |\omega'| \\ \omega' & \text{if } |\omega'| > |\omega| \end{cases}$$

Equation 53 is a perfect differential for F_1 given by

$$F_1 = -\int_{-\infty}^{\infty} \frac{g}{|\omega|} e^{i[(|\omega|\omega/g)\alpha - \omega t]} e^{(\omega^2/g)\delta}\, d\xi_{1(x)}(\omega) \quad (55)$$

Equation 54 can be expressed as a perfect differential if A is chosen to be

$$A = 2t \int_{-\infty}^{\infty} \frac{|\omega^3|}{g} \cdot e^{(2\omega^2/g)\delta}\, d\xi_{1(x)}(\omega)\, d\xi_{1(x)}(-\omega) \quad (56)$$

A was defined in equaton 39.

Hence, the form of the perfect differential is

$$F_2 = \iint_R i(\omega^{**}e^{|\omega^{*2}/g|\delta} - (\omega + \omega')e^{[(\omega^2/g)+(\omega'^2/g)]\delta}) \cdot e^{i[(\omega^{*2}/g)\alpha - (\omega+\omega')t]}\, d\xi_{1(x)}(\omega)\, d\xi_{1(x)}(\omega') \quad (57)$$

The solution for irrotational random long-crested gravity waves in deep water to second order is now complete and is written as

$$X = \alpha + \int_{-\infty}^{\infty} e^{i[(|\omega|\omega/g)\alpha - \omega t]} e^{(\omega^2/g)\delta}\, d\xi_{1(x)}(\omega) + i \iint_R (Ce^{[(\omega^2/g)+(\omega'^2/g)]\delta} - Me^{|\omega^{*2}/g|\delta}) \cdot e^{i[(\omega^{*2}/g)\alpha - (\omega+\omega')t]}\, d\xi_{1(x)}(\omega)\, d\xi_{1(x)}(\omega') + 4t\int_0^{\infty} \frac{\omega^3}{g} e^{2(\omega^2/g)\delta}\, d\xi_{1(x)}(\omega)\, d\xi_{1(x)}(-\omega) \quad (58)$$

$$Z = \delta - i \int_{-\infty}^{\infty} \operatorname{sgn}(\omega) e^{i[(|\omega|\omega/g)\alpha - \omega t]} \cdot e^{(\omega^2/g)\delta} \, d\xi_{1(x)}(\omega) + \iint_R (De^{[(\omega^2/g)+(\omega'^2/g)]\delta} - M \cdot \operatorname{sgn}(\omega + \omega') e^{|\omega^{*2}/g|\delta}) \cdot e^{i[(\omega^{*2}/g)\alpha - (\omega+\omega')t]} \, d\xi_{1(x)}(\omega) \, d\xi_{1(x)}(\omega') + \int_0^{\infty} \frac{2\omega^2}{g} e^{(2\omega^2/g)\delta} \, d\xi_{1(x)}(\omega) \, d\xi_{1(x)}(-\omega) \quad (59)$$

$$P = -\rho g \, \delta - \iint_R \rho g E(e^{|\omega^{*2}|\delta} - e^{[(\omega^2/g)+(\omega'^2/g)]\delta}) e^{i[(\omega^{*2}/g)\alpha - (\omega+\omega')t]} \cdot d\xi_{1(x)}(\omega) \, d\xi_{1(x)}(\omega') \quad (60)$$

where C, D, E, and M are defined by (43), (44), (45), and (49), respectively.

Mass transport and second-order spectrum, cross spectrum, and bispectrum. If the mean position of a particle at the free surface is considered, it can be seen from examination of (58) and (59) that the particle does not remain at its undisturbed position but has a small vertical shift, which can be removed by a coordinate shift

$$\int_0^{\infty} \frac{2\omega^2}{g} S_{1(x)}(\omega) \, d\omega$$

from the mean position, and a horizontal forward velocity

$$\bar{U} = 4 \int_0^{\infty} \frac{\omega^3}{g} e^{2(\omega^2/g)\delta} S_{1(x)}(\omega) \, d\omega \quad (61)$$

Equation 61 is usually called the mass transport velocity (or simply the drift). For a single sine wave, $4S_{(x)}(\omega_0) d\omega$ is, by definition of the spectrum, equal to the square of the amplitude. The expression for the mass transport velocity can then be written as

$$\bar{U} = \frac{\omega_0^3}{g} a^2 e^{2(\omega_0^2/g)\delta}$$

where a is the amplitude. This corresponds to Stokes' result. Since U depends on the first-order X spectrum, $S_{1(x)}(\omega)$, it is necessary to determine the spectrum in order to calculate the mass transport velocity.

If it is assumed that $\xi_{1(x)}(\omega)$ is a Gaussian random process of independent increments with zero mean, the spectrum of the processes

$$X' = X - \bar{X}(= X_1 + X_2 - \bar{X})$$

and

$$Z' = Z - \bar{Z}(= Z_1 + Z_2 - \bar{Z})$$

for any particle in the fluid can be obtained. The spectra of X' and Z' at the free surface are derived as follows.

Set $\delta = 0$ in (58), (59), and (60). This results in

$$X' = \int_{-\infty}^{\infty} e^{i[(|\omega|\omega/g)\alpha - \omega t]} \, d\xi_{1(x)}(\omega) + i \iint_R (C - M) e^{i[(\omega^{*2}/g)\alpha - (\omega+\omega')t]} \cdot d\xi_{1(x)}(\omega) \, d\xi_{1(x)}(\omega') + 4t \int_0^{\infty} \frac{\omega^3}{g} \, d\xi_{1(x)}(\omega) \, d\xi_{1(x)}(-\omega) - 4t \int_0^{\infty} \frac{\omega^3}{g} S_{1(x)}(\omega) \, d\omega \quad (62)$$

$$Z' = -\int_{-\infty}^{\infty} i \operatorname{sgn}(\omega) e^{i[(|\omega|\omega/g)\alpha - \omega t]} \, d\xi_{1(x)}(\omega) + \iint_R [D - M \operatorname{sgn}(\omega + \omega')] e^{i[(\omega^{*2}/g)\alpha - (\omega+\omega')t]} \, d\xi_{1(x)}(\omega) \, d\xi_{1(x)}(\omega') + \int_0^{\infty} \frac{2\omega^2}{g} \, d\xi_{1(x)}(\omega) \, d\xi_{1(x)}(-\omega) - \int_0^{\infty} \frac{2\omega^2}{g} S_{1(x)}(\omega) \, d\omega \quad (63)$$

and

$$R_{(x)}(\tau) = E[X'(t)X'(t+\tau)] = \int_{-\infty}^{\infty} e^{i\omega\tau} S_{1(x)}(\omega) \, d\omega + \iint\iint_R [C(\omega, \omega') - M(\omega, \omega')] \cdot [C(\omega'', \omega''') - M(\omega'', \omega''')] e^{i[(\omega^{*2}/g) - (\omega''^{*2}/g)\alpha - (\omega+\omega'-\omega''-\omega''')t]} \cdot e^{i(\omega''+\omega''')\tau} E[d\xi_{1(x)}(\omega) \, d\xi_{1(x)}(\omega') \, \overline{d\xi_{1(x)}(\omega'') \, d\xi_{1(x)}(\omega''')}] \quad (64)$$

$$R_{(z)}(\tau) = E[Z'(t)Z'(t+\tau)] = \int_{-\infty}^{\infty} e^{i\omega\tau} S_{1(x)}(\omega)\, d\omega$$
$$+ \iint\iint_R [D(\omega, \omega') - M(\omega, \omega') \operatorname{sgn}(\omega + \omega')]$$
$$\cdot [D(\omega'', \omega''') - M(\omega'', \omega''') \operatorname{sgn}(\omega'' + \omega''')] e^{i[(\omega^{*2}/g - \omega''^{*2}/g)\alpha - (\omega + \omega' - \omega'' - \omega''')t]}$$
$$\cdot e^{i(\omega'' + \omega''')\tau} E[d\xi_{1(x)}(\omega)\, d\xi_{1(x)}(\omega')\, \overline{d\xi_{1(x)}(\omega'')\, d\xi_{1(x)}(\omega''')}] \quad (65)$$

The cross-product term is zero since $d\xi_{1(x)}(\omega)$ is assumed to be a Gaussian random variable with zero mean. A further consequence of this assumption is that the expected values of fourfold products of $d\xi_{1(x)}(\omega)$ can be expressed by twofold products [*Isserlis*, 1918].

$$E\{d\xi(\omega_1)\, d\xi(\omega_2)\, d\xi(\omega_3)\, d\xi(\omega_4)\}$$
$$= E\{d\xi(\omega_1)\, d\xi(\omega_2)\} E\{d\xi(\omega_3)\, d\xi(\omega_4)\}$$
$$+ E\{d\xi(\omega_1)\, d\xi(\omega_3)\} E\{d\xi(\omega_2)\, d\xi(\omega_4)\}$$
$$+ E\{d\xi(\omega_1)\, d\xi(\omega_4)\} E\{d\xi(\omega_2)\, d\xi(\omega_3)\} \quad (66)$$

Therefore

$$R_{(x)}(\tau) = \int_{-\infty}^{\infty} e^{i\omega\tau} S_{1(x)}(\omega)\, d\omega$$
$$+ \iint_{-\infty}^{\infty} e^{i(\omega+\omega')\tau} \{[C(\omega, \omega') - M(\omega, \omega')]^2$$
$$+ [C(\omega, \omega') - M(\omega, \omega')]$$
$$\cdot [C(\omega', \omega) - M(\omega', \omega)]\}$$
$$\cdot S_{1(x)}(\omega) S_{1(x)}(\omega')\, d\omega\, d\omega' \quad (67)$$

$$R_{(z)}(\tau) = \int_{-\infty}^{\infty} e^{i\omega\tau} S_{1(x)}(\omega)\, d\omega$$
$$+ \iint_{-\infty}^{\infty} e^{i(\omega+\omega')\tau} \{[D(\omega, \omega')$$
$$- M(\omega, \omega') \operatorname{sgn}(\omega + \omega')]^2$$
$$+ [D(\omega, \omega') - M(\omega, \omega') \operatorname{sgn}(\omega + \omega')]$$
$$\cdot [D(\omega', \omega) - M(\omega', \omega) \operatorname{sgn}(\omega + \omega')]\}$$
$$\cdot S_{1(x)}(\omega) S_{1(x)}(\omega')\, d\omega\, d\omega' \quad (68)$$

Replacing ω' by $\lambda - \omega$ in (67) and (68), one obtains the spectrum of X' and Z' upon taking the Fourier transform.

$$S_{(x)}(\omega) = S_{1(x)}(\omega) + 4 \int_0^{\infty} K(\lambda; \omega) S_{1(x)}(\lambda) S_{1(x)}(\lambda - \omega)\, d\lambda \quad (69)$$

$$S_{(z)}(\omega) = S_{1(x)}(\omega) + 4 \int_0^{\infty} H(\lambda; \omega) S_{1(x)}(\lambda) S_{1(x)}(\lambda - \omega)\, d\lambda \quad (70)$$

where

$$K(\lambda; \omega) = \begin{cases} \left[\dfrac{\lambda^3 - (\omega - \lambda)^3}{\omega} - \lambda(2\lambda - \omega)\right]^2 \Big/ g^2 & \text{for } \lambda > \omega > 0 \\ 0 & \omega > 0, \quad \omega \geq \lambda \end{cases} \quad (71)$$

$$H(\lambda; \omega) = \begin{cases} (\omega - \lambda)^4 / g^2 & \text{for } \lambda > \omega > 0 \\ 0 & \omega > 0, \quad \omega \geq \lambda \end{cases} \quad (72)$$

The remainder of the definition of H and K follows from the symmetry of the spectrum.

The convolutions on the right-hand sides of (69) and (70) are the second-order spectrum corrections due to the nonlinear effects. The effect of the function $K(\lambda; \omega)$ on the second-order term in the X spectrum is to provide high spectral values around the origin, $\omega = 0$. The function $H(\lambda; \omega)$ contributes little to the Z spectrum because it does not have any singularities.

Since the second-order correction of the Z spectrum is small in comparison with the first-order X spectrum, it is reasonable to say that the Z spectrum is approximately equal to the first-order X spectrum, $S_{1(x)}(\omega)$. Therefore, one can replace $S_{1(x)}(\omega)$ by $S_{(z)}(\omega)$ in (61). The mass transport velocity

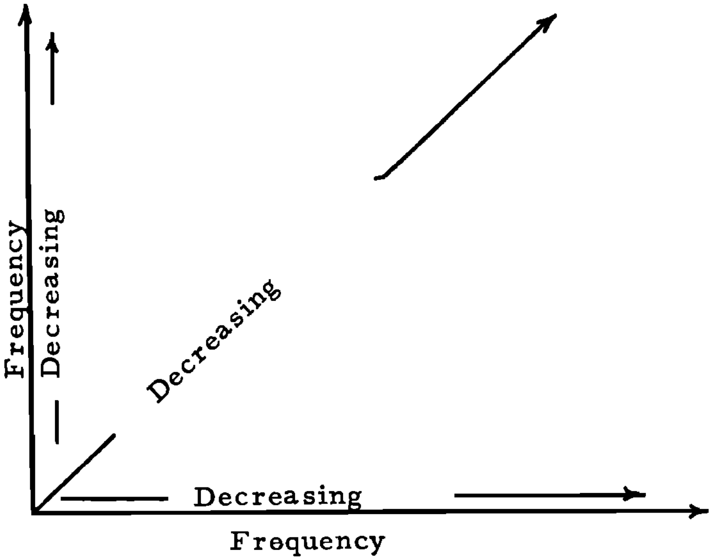

$$\bar{U} = 4 \int_0^\infty \frac{\omega^3}{g} e^{(2\omega^2/g)\delta} S_{1(z)}(\omega)\, d\omega$$

$$\cong 4 \int_0^\infty \frac{\omega^3}{g} e^{(2\omega^2/g)\delta} S_{(z)}(\omega)\, d\omega \qquad (73)$$

can then be evaluated from an estimated spectrum of the vertical motion. Also, from these aspects of the X spectrum and Z spectrum, the

$$J(\lambda; \omega) = \begin{cases} 0 & \text{if} \quad 0 < \lambda < \omega \\ \left(2\frac{\lambda}{\omega} - 1\right)(\lambda - \omega)^4 & \text{if} \quad 0 < \omega < \lambda \\ \left(1 - 2\frac{\lambda}{\omega}\right)\lambda^4 & \text{if} \quad 0 > \lambda\ 0 < \omega \end{cases} \qquad (75)$$

bispectrum of the horizontal motion is expected to have a relatively high value over the low $\omega\omega'$ plane and to decrease diagonally toward the high $\omega\omega'$ plane. The accompanying diagram shows the expected nature of the X bispectrum. The Z bispectrum is expected to have low values over the whole $\omega\omega'$ plane, because of the assumption of a Gaussian distribution in $d\xi_{1(x)}(\omega)$ and the small second-order correction in Z.

The cross spectrum of the motion of a particle between the X and Z coordinates can be derived in a similar manner. It is obtained as

$$Cr(\omega) = i(Qr_1(\omega) + Qr_2(\omega))$$

$$= i\left(S_{1(z)}(\omega) + \frac{2}{g^2}\int_{-\infty}^{\infty} J(\lambda; \omega) \cdot S_{1(z)}(\lambda) S_{1(z)}(\lambda - \omega)\, d\lambda\right) \qquad (74)$$

where $Cr(\omega)$ is the cross spectrum, $Qr_1(\omega)$ is the first-order quadrature spectrum, and $Qr_2(\omega)$ is the second-order quadrature spectrum.

Hence the cross spectrum consists only of the quadrature spectrum, and it is almost the same as the first-order X spectrum in the high-frequency range. The second-order correction in the cross spectrum is significant in the low-frequency region, but it is still very small in comparison with the second-order correction to the X spectrum.

Viscous Flow

Governing equations. If the functions $x = x(\alpha, \delta, t)$ and $z = z(\alpha, \delta, t)$ are assumed to be invertible, it is possible to express α and δ in terms of x and z (where $\alpha = \alpha(x, z, t)$ and

$\delta = \delta(x, z, t)$). For a given function $F(x, z, t)$, then, there must exist another function $f(\alpha, \delta, t)$ such that

$$F(x, z, t) = f(\alpha, \delta, t)$$

where α and δ are functions of x, z, and t.

Hence the derivatives of the function F with respect to x and z can be related to the derivatives of f with respect to α and δ by

$$\frac{\partial F}{\partial x} = J\left(\frac{f, z}{\alpha, \delta}\right) \Big/ J\left(\frac{x, z}{\alpha, \delta}\right)$$
$$\frac{\partial F}{\partial z} = J\left(\frac{x, f}{\alpha, \delta}\right) \Big/ J\left(\frac{x, z}{\alpha, \delta}\right) \tag{76}$$

If $J(x, z/\alpha, \delta)$ is equal to unity, the above equations reduce to

$$\partial F/\partial x = J(f, z/\alpha, \delta) \tag{77}$$

$$\partial F/\partial z = J(x, f/\alpha, \delta) \tag{78}$$

It can be seen that the viscous terms in the Eulerian equations of motion can be transformed into Lagrangian coordinates by use of (77) and (78), if the fluid is assumed to be incompressible (see also *Pierson* [1962] and *Corrsin* [1961]). This results in

$$\nu\nabla^2 U(x, z, t) = \nu\left[J\left(\frac{J(u, z/\alpha, \delta), z}{\alpha, \delta}\right) + J\left(\frac{x, J(x, u/\alpha, \delta)}{\alpha, \delta}\right)\right] = \nu[FU(\alpha, \delta, t) + GU(\alpha, \delta, t)] \tag{79}$$

and

$$\nu\nabla^2 W(x, z, t) = \nu\left[J\left(\frac{J(w, z/\alpha, \delta), z}{\alpha, \delta}\right) + J\left(\frac{x, J(x, w/\alpha, \delta)}{\alpha, \delta}\right)\right] = \nu[FW(\alpha, \delta, t) + GW(\alpha, \delta, t)] \tag{80}$$

for the Navier-Stokes terms in the Eulerian equations. In (79) and (80) ν is the kinematic viscosity and ∇^2 is the Laplace operator.

The equation of motion for viscous flow can then be stated as

$$X_{tt}X_\alpha - \nu(FU + GU)X_\alpha + (Z_{tt} + g)Z_\alpha - \nu(FW + GW)Z_\alpha + \frac{P_\alpha}{\rho} = 0 \tag{81}$$

$$X_{tt}X_\delta - \nu(FU + GU)X_\delta + (Z_{tt} + g)Z_\delta - \nu(FW + GW)Z_\delta + \frac{P_\delta}{\rho} = 0 \tag{82}$$

Upon linearizing equations 81 and 82 and the continuity equation in the same manner as that for the nonviscous equations, one obtains

ϵ equations

$$X_{1tt} + gZ_{1\alpha} + \frac{P_{1\alpha}}{\rho} = \nu(X_{1t\alpha\alpha} + X_{1t\delta\delta}) \tag{83}$$

$$Z_{1tt} + gZ_{1\delta} + \frac{P_{1\delta}}{\rho} = \nu(Z_{1t\alpha\alpha} + Z_{1t\delta\delta}) \tag{84}$$

$$X_{1\alpha} + Z_{1\delta} = 0 \tag{85}$$

ϵ^2 equations

$$\begin{aligned} X_{2tt} + gZ_{2\alpha} + P_{2\alpha}/\rho - \nu(X_{2t\alpha\alpha} + X_{2t\delta\delta}) &= -X_{1tt}X_{1\alpha} - Z_{1tt}Z_{1\alpha} \\ &+ \nu[(X_{1t\alpha\alpha} + 3X_{1t\delta\delta})X_{1\alpha} \\ &+ 2X_{1t\alpha\alpha}Z_{1\delta} + X_{1t\alpha}(Z_1\alpha_\delta - X_{1\delta\delta}) \\ &- 2X_{1t\alpha\delta}(Z_{1\alpha} + X_{1\delta}) \\ &- X_{1t\delta}(Z_{1\alpha\alpha} - X_{1\alpha\delta}) \\ &+ (Z_{1t\alpha\alpha} + Z_{1t\delta\delta})Z_{1\alpha}] \end{aligned} \tag{86}$$

$$\begin{aligned} Z_{2tt} + gZ_{2\delta} + P_{2\delta}/\rho - \nu(Z_{2t\alpha\alpha} + Z_{2t\delta\delta}) &= -X_{1tt}X_{1\delta} - Z_{1tt}Z_{1\delta} \\ &+ \nu[(X_{1t\alpha\alpha} + X_{1t\delta\delta})X_{1\delta} \\ &+ (Z_{1t\alpha\alpha} + Z_{1t\delta\delta})Z_{1\delta} + 2Z_{1t\alpha\alpha}Z_{1\delta} \\ &+ 2Z_{1t\delta\delta}X_{1\alpha} + Z_{1t\alpha}(Z_{1\alpha\delta} - Z_{1\delta\delta}) \\ &- 2Z_{1t\alpha\delta}(Z_{1\alpha} + X_{1\delta}) \\ &- Z_{1t\delta}(Z_{1\alpha\alpha} - X_{1\alpha\delta})] \end{aligned} \tag{87}$$

$$X_{2\alpha} + Z_{2\delta} + Z_{1\delta}X_{1\alpha} - X_{1\delta}Z_{1\alpha} = 0 \tag{88}$$

Boundary conditions. To derive the boundary conditions at a free surface, consider the balance of forces on a small triangular element just beneath the surface of a general fluid. The vertical and horizontal balance of forces (for details, see *Kinsman* [1965]) are given, respectively, by

$$-(P_0 + K\mathfrak{T})\, dS \cos\theta + \tau\, dS \sin\theta = P^{zz}\, dS \cos\theta + P^{xz}\, dS \sin\theta \tag{89}$$

$$(P_0 + K\mathfrak{T})\, dS \sin\theta + \tau\, dS \cos\theta = P^{xz}\, dS \cos\theta - P^{xx}\, dS \sin\theta \tag{90}$$

where

P_0 = pressure at the surface.
K = curvature.
$\mathfrak{T}$ = surface tension.
τ = tangential surface stress.

Now, for a free surface, $P_0=0$ and $\tau = 0$ at $\delta = 0$. Hence, if the vertical position of the particle is given by $Z(\alpha)$ and the surface tension $\mathfrak{T}$ is neglected, equations 89 and 90 become, respectively,

$$P^{zz}X_\alpha + P^{xz}Z_\alpha = 0 \quad \text{at} \quad \delta = 0 \tag{91}$$

$$P^{zx}X_\alpha - P^{xx}Z_\alpha = 0 \quad \text{at} \quad \delta = 0 \tag{92}$$

However, for a Newtonian fluid,

$$P^{zz} = -p + 2\rho\nu[X_\alpha Z_{t\delta} - Z_{t\alpha}X_\delta] \tag{93}$$

$$P^{xx} = -p + 2\rho\nu[X_{t\alpha}Z_\delta - X_{t\delta}Z_\alpha] \tag{94}$$

$$P^{xz} = P^{zx} = \rho\nu[X_\alpha X_{t\delta} + Z_{t\alpha}Z_\delta - Z_{t\delta}Z_\alpha - X_\delta X_{t\alpha}] \tag{95}$$

Since water can be approximated by a Newtonian fluid, the boundary condition at the free surface ($\delta = 0$) can be obtained by substituting (93), (94), and (95) into (91) and (92). These substitutions result in

$$[-P + 2\rho\nu(X_\alpha Z_{t\delta} - Z_{t\alpha}X_\delta)]X_\alpha + \rho\nu[(X_\alpha X_{t\delta} - X_\delta X_{t\alpha}) + (Z_{t\alpha}Z_\delta - Z_{t\delta}Z_\alpha)]Z_\alpha = 0 \quad \text{at} \quad \delta = 0 \tag{96}$$

$$\rho\nu[(X_\alpha X_{t\delta} - X_\delta X_{t\alpha}) + (Z_{t\alpha}Z_\delta - Z_{t\delta}Z_\alpha)]X_\alpha + [P - 2\rho\nu(X_{t\alpha}Z_\delta - X_{t\delta}Z_\alpha)]Z_\alpha = 0 \quad \text{at} \quad \delta = 0 \tag{97}$$

Upon linearizing the above equations, one finally obtains first-order boundary conditions

$$-P_1 + 2\rho\nu Z_{1t\delta} = 0$$
$$Z_{1t\alpha} + X_{1t\delta} = 0 \quad \text{at} \quad \delta = 0 \tag{98}$$

and second-order boundary conditions

$$P_2 + P_1X_{1\alpha} - 2\rho\nu(Z_{2t\delta} + 2Z_{1t\delta}X_{1\alpha} - X_{1\delta}Z_{1t\alpha}) + \rho\nu(Z_{1t\alpha}Z_{1\alpha} + X_{1t\delta}Z_{1\alpha}) = 0 \quad \text{at} \quad \delta = 0 \tag{99a}$$

$$P_1Z_{1\alpha} - 2\rho\nu X_{1t\alpha}Z_{1\alpha} + \rho\nu(Z_{1t\alpha}Z_{1\delta} + Z_{1t\alpha}X_{1\alpha} + Z_{2t\alpha} - Z_{1t\delta}Z_{1\alpha} + 2X_{1t\delta}X_{1\alpha} + X_{2t\delta} - X_{1\delta}X_{1t\alpha}) = 0 \quad \text{at} \quad \delta = 0 \tag{99b}$$

First-order solution. The method of obtaining the general solution of the above system is the same as for the irrotational case. The first-order solutions can be written as

$$X_1 = \iint_{-\infty}^{\infty} e^{i(k\alpha-\omega t)}e^{|k|\delta}\, d\xi_{1(x)}(\omega, k) + \iint_{-\infty}^{\infty} e^{i(k\alpha-\omega t)}e^{\beta\delta}\, d\xi'_{1(x)}(\omega, k) \tag{100}$$

$$Z_1 = \iint_{-\infty}^{\infty} -i\frac{k}{|k|}e^{i(k\alpha-\omega t)}e^{|k|\delta}\, d\xi_{1(x)}(\omega, k) - \iint_{-\infty}^{\infty} i\frac{k}{\beta}e^{i(k\alpha-\omega t)}e^{\beta\delta}\, d\xi'_{1(x)}(\omega, k) \tag{101}$$

$$P_1 = \iint_{-\infty}^{\infty} i\frac{\rho}{k}[(\omega^2 - g|k|)e^{i(k\alpha-\omega t)}\cdot e^{|k|\delta}]\, d\xi_{1(x)}(\omega, k) + \iint_{-\infty}^{\infty} i\rho\frac{gk}{\beta}e^{i(k\alpha-\omega t)}e^{\beta\delta}\, d\xi'_{1(x)}(\omega, k) \tag{102}$$

where

$$\beta = \left[k^2 + (1-i)^2 \frac{\omega}{2\nu}\right]^{1/2}$$

Substituting the above equations into boundary condition 98, one obtains

$$\frac{i}{k\nu}\left[(\omega^2 - g\,|k|\,)\,d\xi_{1(x)}(\omega, k) - g\frac{k^2}{\beta}\,d\xi'_{1(x)}(\omega, k)\right] - 2\omega k\,d\xi_{1(x)}(\omega, k) - 2\omega k\,d\xi'_{1(x)}(\omega, k) = 0 \qquad (103)$$

$$|k|\,d\xi_{1(x)}(\omega, k) + \beta\,d\xi'_{1(x)}(\omega, k) + \frac{k^2}{\beta}\,d\xi'_{1(x)}(\omega, k) = 0 \qquad (104)$$

Hence,

$$d\xi'_{1(x)}(\omega, k) = \frac{2\,|k|}{(k^2/\beta) - \beta}\,d\xi_{1(x)}(\omega, k) \qquad (105)$$

$$\omega^2 - g\,|k| - k^2\omega^2\left(\frac{2\nu}{i\omega}\right) - \left[g\frac{k^2}{\beta} + k^2\omega^2\left(\frac{2\nu}{i\omega}\right)\right]\frac{2\,|k|\,\beta}{k^2 - \beta^2} = 0 \qquad (106)$$

For surface waves on water, the ratio $\omega/2\nu k^2$ is very large. For the shortest wave, for example, $k = 3.8\ \text{cm}^{-1}$ and $\nu = 0.01\ \text{cm}^2\ \text{sec}^{-1}$, one has $(\omega/2\nu k^2) \cong 280$. Therefore, it is safe to make the following approximation:

$$\frac{\beta}{k} = \left[1 + (1-i)^2\frac{\omega}{2\nu k^2}\right]^{1/2} \cong (1-i)\left(\frac{\omega}{2\nu k^2}\right)^{1/2} \gg 1$$

On neglecting the higher-order terms of k/β in (105) and (106) one obtains

$$\omega^2 \cong g\,|k|\,(1 - 2ik^2l^2) \cong g\,|k|\,(1 - 2ik^2l^2 - k^4l^4) = (\omega_{(R)} + i\omega_{(I)})^2 \qquad (107)$$

$$\frac{d\xi'_{1(x)}(\omega, k)}{d\xi_{1(x)}(\omega, k)} = -\frac{2\,|k|}{\beta[(k^2/\beta^2) - 1]} \qquad (108)$$

where

$$l = [2\nu/\,|\omega_{(R)}|\,]^{1/2}$$

$$\beta \cong \begin{cases}(1-i)\dfrac{1}{l} & \text{if}\quad \omega > 0\\[2mm] (1+i)\dfrac{1}{l} & \text{if}\quad \omega < 0\end{cases}$$

The expressions for first order, then, become

$$X_1 = \int_{-\infty}^{\infty} e^{-|\omega|k^2l^2t} e^{i[(|\omega|\omega/g)\alpha - \omega t]} \cdot\left[e^{(\omega^2/g)\delta} - \frac{2\,|k|}{\beta}e^{\beta\delta}\right] d\xi_{1(x)}(\omega) \qquad (109)$$

$$Z_1 = \int_{-\infty}^{\infty} e^{-|\omega|k^2l^2t} e^{i[(|\omega|\omega/g)\alpha - \omega t]} \cdot\left[-i\frac{k}{|k|}e^{(\omega^2/g)\delta} - i\frac{2k\,|k|}{\beta^2}e^{\beta\delta}\right] d\xi_{1(x)}(\omega) \qquad (110)$$

$$P_1 = \int_{-\infty}^{\infty} e^{-|\omega|k^2l^2t} e^{i[(|\omega|\omega/g)\alpha - \omega t]} \cdot\left[-i\frac{\rho}{k}(\omega^2 - g\,|k|\,)e^{(\omega^2/g)\delta} + i\rho\frac{2gk\,|k|}{\beta^2}e^{\beta\delta}\right] d\xi_{1(x)}(\omega) \qquad (111)$$

where (R) is dropped from $\omega_{(R)}$ for convenience and where the last term in each bracket of (110) may be neglected.

Second-order solution. Substitution of the first-order solutions into the second-order differential equations 86, 87, and 88 and the boundary conditions 99 yields

$$X_2 = \iint_R e^{-ct}[A_1e^{|k+k'|\delta} + A_2e^{(|k|+k')\delta} + A_3e^{(|k|+\beta')\delta}]e^{i[(k+k')\alpha]}e^{-i(\omega+\omega')t} \cdot d\xi_{1(x)}(\omega)\,d\xi_{1(x)}(\omega') + M_{\nu2(x)} \qquad (112)$$

$$Z_2 = \iint_R e^{-ct}[B_1e^{|k+k'|\delta} + B_2e^{(|k|+|k'|)\delta} + B_3e^{(|k|+\beta')\delta}]e^{i[(k+k')\alpha]}e^{-i(\omega+\omega')t} \cdot d\xi_{1(x)}(\omega)\,d\xi_{1(x)}(\omega') + M_{\nu2(z)} \qquad (113)$$

where the higher-order terms of k/β have been neglected and the other constants are defined as

$$c = 2\nu(k^2 + k'^2) \qquad (114)$$

$$A_1 = \frac{-i}{g^2 |k + k'|} \cdot \frac{|\omega^5| + |\omega^3| \omega'^2 + |\omega'^3| \omega^2 + |\omega'^5|}{\omega + \omega'} \quad (115)$$

$$A_2 = i \frac{|\omega^3| + |\omega'^3|}{g(\omega + \omega')} \quad (116)$$

$$A_3 = \frac{-i}{\beta_2'} \frac{2k |k'| (\omega^2 - \omega\omega' + 2\omega'^2)}{(\omega + \omega')\omega'} \quad (117)$$

$$B_1 = -iA_1 \frac{k + k'}{|k + k'|} \quad (118)$$

$$B_2 = (\omega^2 - \omega\omega' + \omega'^2)/g \quad (119)$$

$$B_3 = -2 |kk'| /\beta_2' \quad (120)$$

$$M_{v2(x)} = 4 \int_0^\infty \frac{1}{c} (1 - e^{-ct}) \left[\omega k e^{2k\delta} - 2\omega k^2 l \left(\sin \frac{1}{l} \delta + \cos \frac{1}{l} \delta \right) e^{(k+1/l)\delta} + \omega k \sin 2k\delta \right] d\xi_{1(x)}(\omega)\, d\xi_{1(x)}(-\omega) \quad (121)$$

$$M_{v2(z)} = \int_0^\infty 2e^{-ct} k e^{2k\delta} \cdot d\xi_{1(x)}(\omega)\, d\xi_{1(x)}(-\omega) \quad (122)$$

Hence, the motion of a particle is damped exponentially with time by viscous effects. The motion will then be approximately at rest again after a certain time. Since water waves have quite small c; $k = 1$, $c = 0.02$, and $k = 0.1$, $c = 0.0002$, the damping is slow and can be neglected if the time interval under analysis is smaller than a few minutes.

Mass transport gradient. If $ct \ll 1$, then, by neglecting the higher-order terms of ct, one has

$$M_{v2(x)} = 4 \int_0^\infty t \left[\omega k e^{2k\delta} - 2\omega k^2 l \left(\sin \frac{1}{l} \delta + \cos \frac{1}{l} \delta \right) e^{(k+1/l)\delta} + \omega k \sin 2k\delta \right] d\xi_{1(x)}(\omega)\, d\xi_{1(x)}(-\omega)$$

At the free surface ($\delta = 0$), this becomes

$$M_{v2(x)} = 4 \int_0^\infty t(\omega k - 2\omega k^2 l)\, d\xi_{1(x)}(\omega)\, d\xi_{1(x)}(-\omega) \cong 4 \int_0^\infty t\omega k\, d\xi_{1(x)}(\omega)\, d\xi_{1(x)}(-\omega) = M_{v2(x)}$$

Hence, the surface mass transport velocity at the free surface for the viscous solution is nearly the same as that of the nonviscous solution.

The gradient of the mass transport velocity near the free surface is

$$E[\partial U/\partial \delta] \cong 16 \int_0^\infty \omega k^2 S_{1(x)}(\omega)\, d\omega \quad (123)$$

which is twice as large as the result for the irrotational solution and agrees with the results of *Longuet-Higgins* [1953]. This implies that, if one is interested only in the mass transport velocity at the free surface, the motion can be considered to be irrotational. If the mass transport gradient is considered, the viscous effect cannot be neglected.

Experimental Results

Description of experiment and data. In 1962 a water tank experiment to determine the position of a particle on a water surface subjected to a train of artificially generated waves was performed at the Stevens Institute of Technology under the direction of John F. Dalzell. The data obtained from this experiment can be used to verify parts of the above theoretical results. A brief description of this experiment will be given here. *Pierson* [1962] gives additional details on the experiment.

Small wooden balls (0.50 cm in diameter) were placed on the water surface of a water-filled tank (dimensions, 92 × 1.8 × 3.6 meters) to represent typical fluid particles. Long-crested random waves were then generated at one end of the tank while the motions of the particles were tracked by an optical-photographic instrument. Thus, the floating positions of the spheres in X, Y, and Z Cartesian coordinates were determined as a function of time from the films.

The optical-photographic instrument consisted of a mirror, strobe lights, an Airiflex 35-mm camera, and an electric timing device, mounted on a moving carriage and 100 feet of Keuffel and Esser tape. The apparatus is illustrated in Figure 1a. The camera, with a 28-mm Schneider

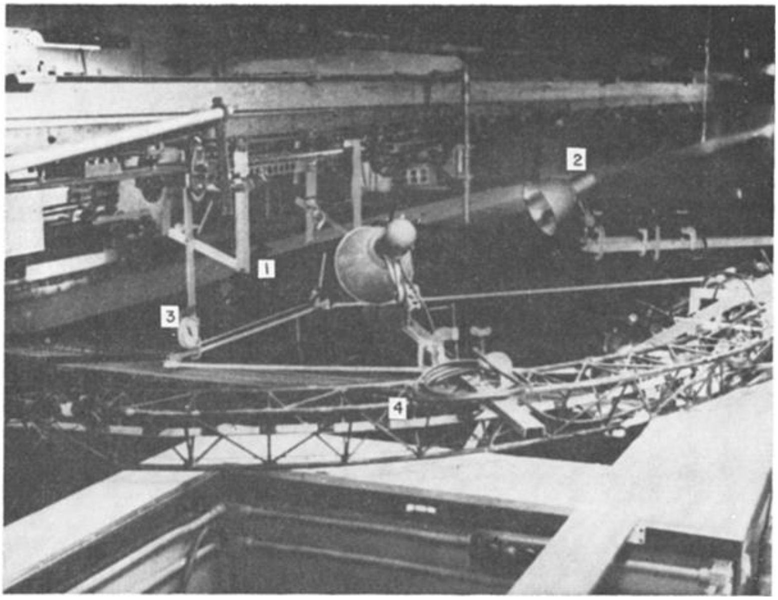

Fig. 1*a*. Design of experimental apparatus. (1) mirror, (2) strobe light, (3) timing device, and (4) carriage.

lens attached, was synchronized with the strobe light to take 10 frames per second. The mirror with a zero-line indicator was mounted in front of the camera at a 45° angle, so that the camera would see the mirror in the top half of each frame. This is similar to viewing the balls from directly overhead. Figure 1*b* is a sample photograph from this experiment. The white spot labeled a represents a ball on the water surface and the one labeled b is the mirror image

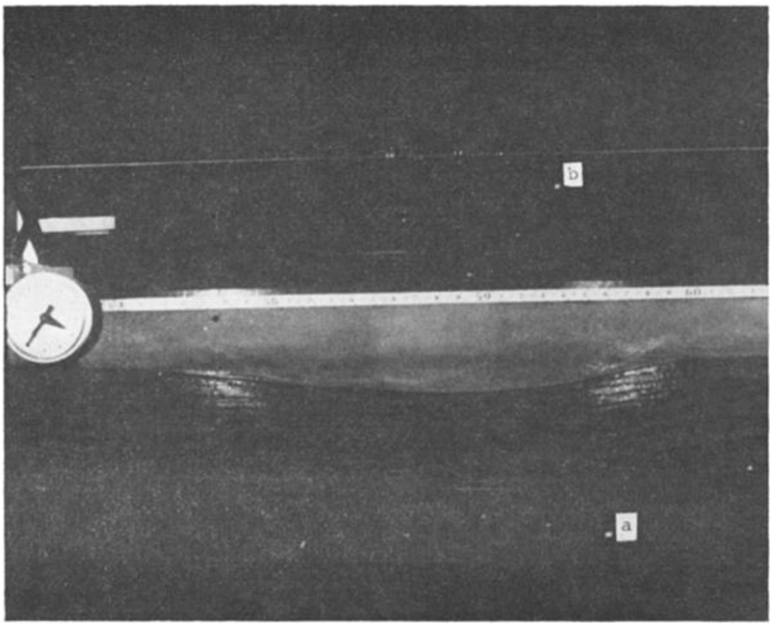

Fig. 1*b*. Sample photo of the ball on the wave surface and its image in the mirror.

of a. In the mirror view, the balls moved mostly to the left and right, to provide data on the X and Y components of the fluid motion (the motion normal to X was small). The X and Z motions of the balls were recorded in the lower half of the frame. An electric clock was placed on the lower right-hand side of the mirror frame to identify the films. One end of the 100 feet of Keuffel and Esser tape was fastened to the edge of one end of the tank. It was then passed along rollers on the camera transport, beneath the mirror and along the length of the tank, where it was then spring-loaded to a tension of 5 pounds. The point-positions of the sphere were digitized at Aero Service Corporation, Philadelphia, under the direction of David S. Fuller by the use of a specially constructed reticle that was placed over the film frame and yielded readings of high accuracy when viewed with a stereomicroscope.

The entire experiment yielded 24 sets of data. Each set consisted of three series of data representing the simultaneous X, Y, and Z coordinates of a ball. The coordinate position sampling time was 0.1 second, and the length of a particular set of data varied from 20 to 100 seconds, depending on experimental conditions. Figure 2 shows graphs of one of the longest sets of data.

A motion picture has been made from a composite of these photographs to give a general idea of the motion of a particle on a surface subjected to a series of long-crested random waves. This film may be of special interest to those studying the problems of breaking waves [*Pierson*, 1963].

Under the assumption that the horizontal position $X(t)$ of the sphere at a given time t after initial time t_0 is an algebraic sum of the initial position $X(0)$, the horizontal displacement due to the oscillatory part of the wave motion $X_p(t)$, and the product of the mean velocity and time t, i.e.,

$$X(t) = X(0) + Vt + X_p(t)$$

the mean mass transport velocity for each set of data was evaluated by a least-squares method to minimize $\Sigma[X_p(t)]^2$. That is,

$$V = \frac{n[\sum tX(t)] - [\sum X(t)][\sum t]}{n[\sum t^2] - [\sum t]^2} \tag{124}$$

$$X(0) = \frac{[\sum t^2][\sum X(t)] - [\sum t][\sum (tX(t))]}{n[\sum t^2] - [\sum t]^2} \tag{125}$$

After calculation of V and $X(0)$, $X(0) + Vt$ and $\overline{Z(t)}$ were subtracted from the data $X(t)$ and $Z(t)$, respectively. Then the X spectrum and the Z spectrum were calculated for each set of these experimental data with the drift in X and the mean of Z removed. The X and Z bispectra and the cross spectrum between X and Z were also estimated.

Comparison of theoretical and observed spectra. The twenty-four pairs of X and Z spectra calculated in this manner appear to have one particular property. There are high spectral values over the low-frequency region of the X spectrum but not in the Z spectrum. Figure 3 is the same as Figure 2 except for the removal of the drift. Figure 4 is the spectrum corresponding to Figure 3. The big difference between the X spectrum and the Z spectrum over the frequency region below 0.3 sec^{-1} is clearly shown in the spectral curves. Actually, this low-frequency oscillation in the X coordinate can even be seen from Figure 3.

It was then interesting to investigate whether the theoretical model would explain this feature. During the experiment, the wave heights at the 50.7- and 27.0-foot marks on the tape were also recorded every tenth of a second by using a Sanborn two-channel recorder. Recording was started when the first wave passed the 50.7-foot mark and stopped when the camera was switched off. The wave probes were calibrated before and after the experiment by curve fitting.

Tick [1959] showed that the surface wave spectrum of random waves to the second order is approximately the same as the first order except for a small correction over the high-frequency region and small values at low frequencies that, for this purpose, can be set equal to zero. Thus, a theoretical X spectrum and a theoretical Z spectrum were calculated according to (69) and (70) by taking the surface spectrum as a first-order X spectrum. These curves are shown in Figure 5. The curves show good agreement between theory and observations (Figure 4). The ratio $\Sigma S_{(z)}(\omega)/\Sigma S_{(x)}(\omega)$ is also given in the figure. This indicates the

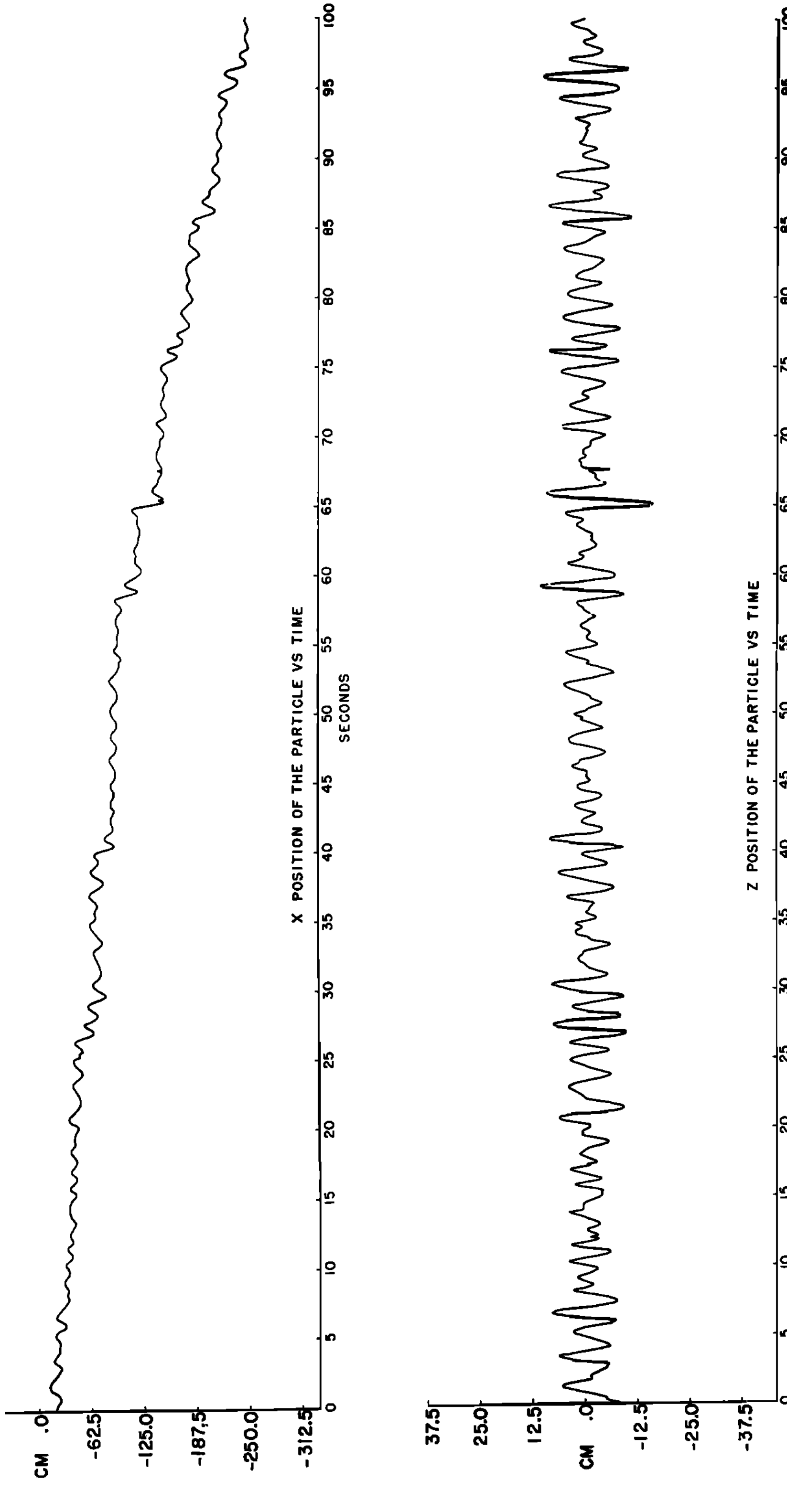

Fig. 2. Sample record of particle position obtained by drawing a smooth curve through points 0.1 second apart.

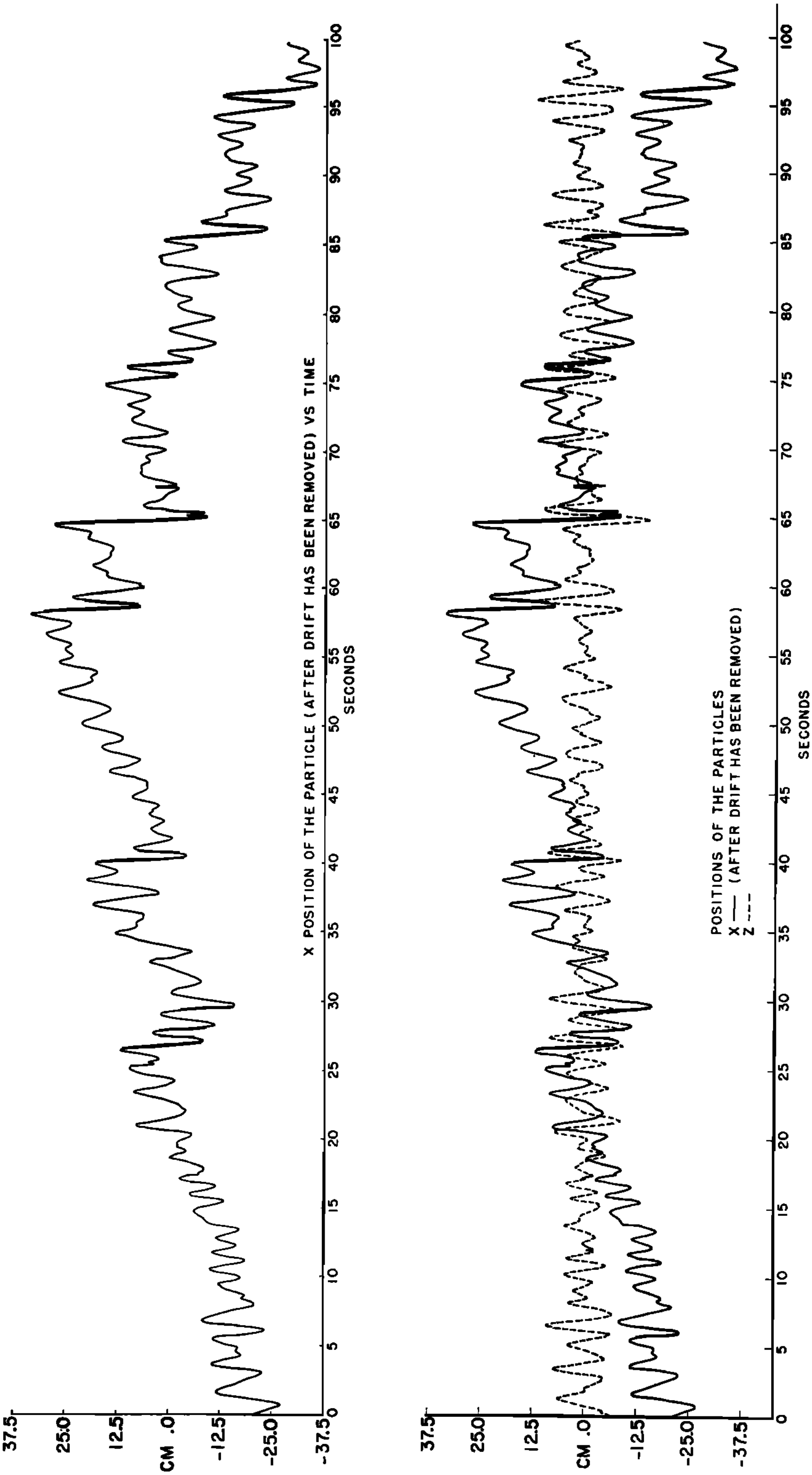

Fig. 3. Sample of particle position after the removal of drift obtained from Figure 2.

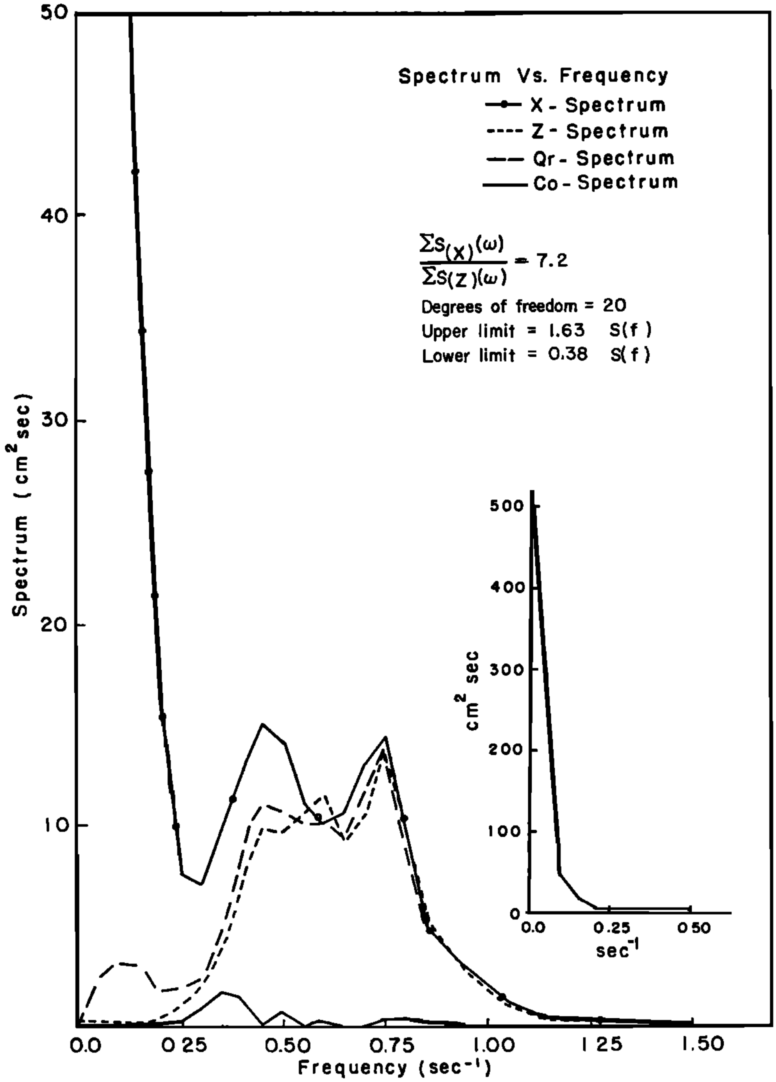

Fig. 4. Corresponding spectra and cross spectra of Figure 3.

importance of the second-order correction. Usually, a large second-order correction is taken as an improper solution and an indication that the solution is diverging. However, the large second-order effect is both observed and correctly explained theoretically in this investigation.

Comparison of theoretical and observed cross spectra. The estimated cross spectra consist of both a quadrature spectrum and a co-spectrum. The quadrature spectrum is almost the same as the spectra of both X and Z over the high-frequency region and has a significant value over the low-frequency band, but it is not comparable to the X spectrum over this region. The co-spectrum is very low over the whole frequency range. It is one order of magnitude smaller than the quadrature spectrum. Figure 4 also shows the corresponding cross spectrum for that run.

The theoretical cross spectrum has been derived and calculated from the surface wave spectrum, which has been discussed previously. It is shown in Figure 5. The estimated and theoretical quadrature spectra show good agreement. The theoretical co-spectrum is equal to

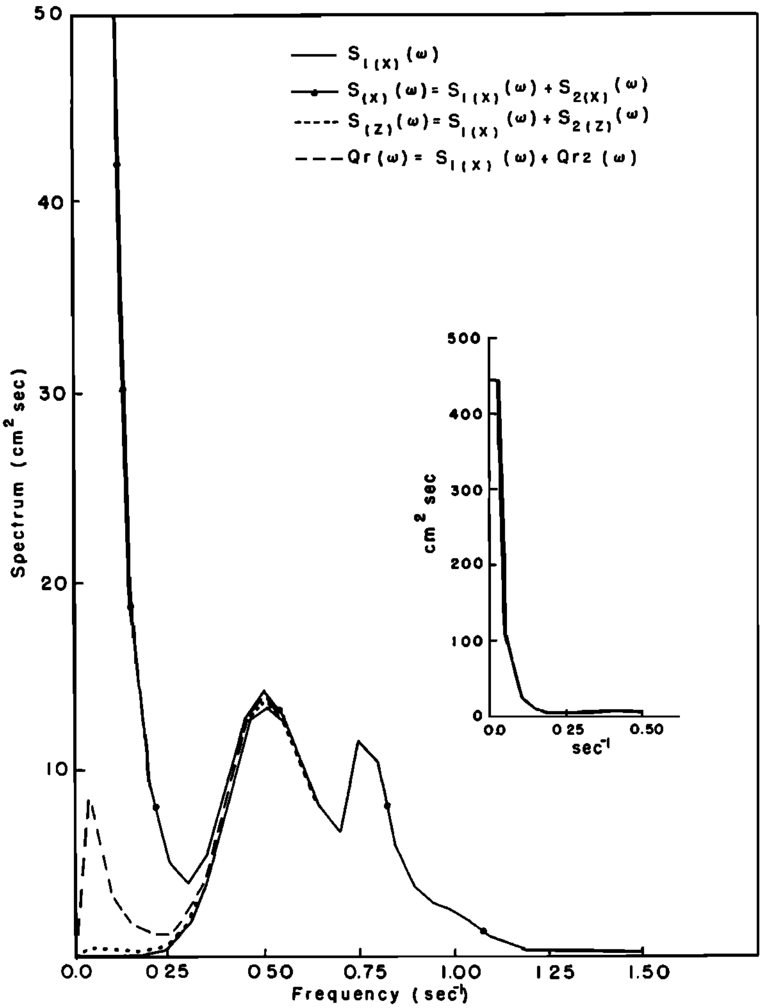

Fig. 5. Theoretically calculated spectrum and cross spectrum from estimated surface wave spectrum.

zero for all frequencies. The actual observed co-spectrum shows a rather small value, however, which may be due either to noise or to sampling variation.

Comparison of theoretical and observed drift. Theoretical mass transport velocities for each set of data were evaluated according to (73) by using the estimated spectrum of Z in that run as an approximation to the first-order spectra of X and Z. The resulting observed values (calculated according to equation 124) and theoretical values for these twenty-four sets of data are given in Table 1 and plotted as a scatter diagram in Figure 6. The averages of the observed and theoretical mass transport velocities are 2.64 and 2.72 cm sec^{-1}, respectively, when the data are weighted according to the length of the run. The theoretical drift calculated from the estimated surface spectrum is 2.77 cm sec^{-1}. The correlation coefficient between them is 0.76. This shows that the observed drift for a small sample of data is correlated with the integral of the product of frequency cubed and the vertical displacement spectrum estimated from that sample. A higher observed drift is associated with a higher value of the integral. The variation of sampling length and the least-squares technique used to evaluate the observed drifts are believed to be responsible for the scatter of the data points.

TABLE 1. Theoretical and Observed Drift

Run Number	Length of Run, sec	Observed Drift, cm/sec	Theoretical Drift, cm/sec
1	20.0	2.19	1.71
2	25.1	1.52	2.64
3	20.0	1.37	2.12
4	39.5	2.48	3.12
5	21.5	2.27	2.20
6	35.8	1.80	2.12
7	29.3	2.30	2.27
8	29.6	2.44	1.97
9	21.8	2.25	2.21
10	22.7	3.29	3.36
11	100.0	2.25	2.74
12	100.0	3.11	3.29
13	30.7	3.03	2.97
14	58.4	3.63	3.00
15	16.5	0.56	1.11
16	33.0	3.05	2.68
17	23.7	2.08	2.42
18	60.4	3.38	3.64
19	33.1	2.01	2.66
20	62.3	4.27	3.23
21	20.8	0.79	1.57
22	25.8	2.25	3.58
23	45.0	1.24	1.74
24	92.5	3.06	2.63
Sum	967.5		

$$\text{Average Observed Drift} = \frac{\sum (\text{Length of Run} \times \text{Observed Drift})}{\sum (\text{Length of Run})} = 2.64 \text{ cm/sec}$$

$$\text{Average Theoretical Drift} = \frac{\sum (\text{Length of Run} \times \text{Theoretically Cal. Drift})}{\sum (\text{Length of Run})}$$

$$= 2.72 \text{ cm/sec}$$

Correction Coefficient = 0.76

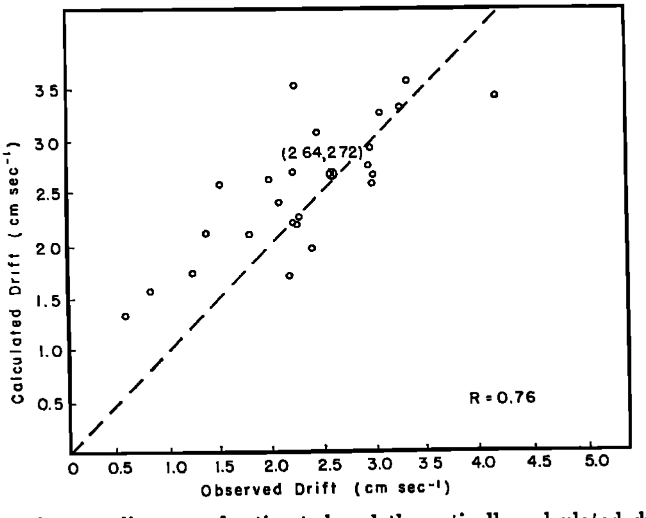

Fig. 6. Scatter diagram of estimated and theoretically calculated drifts.

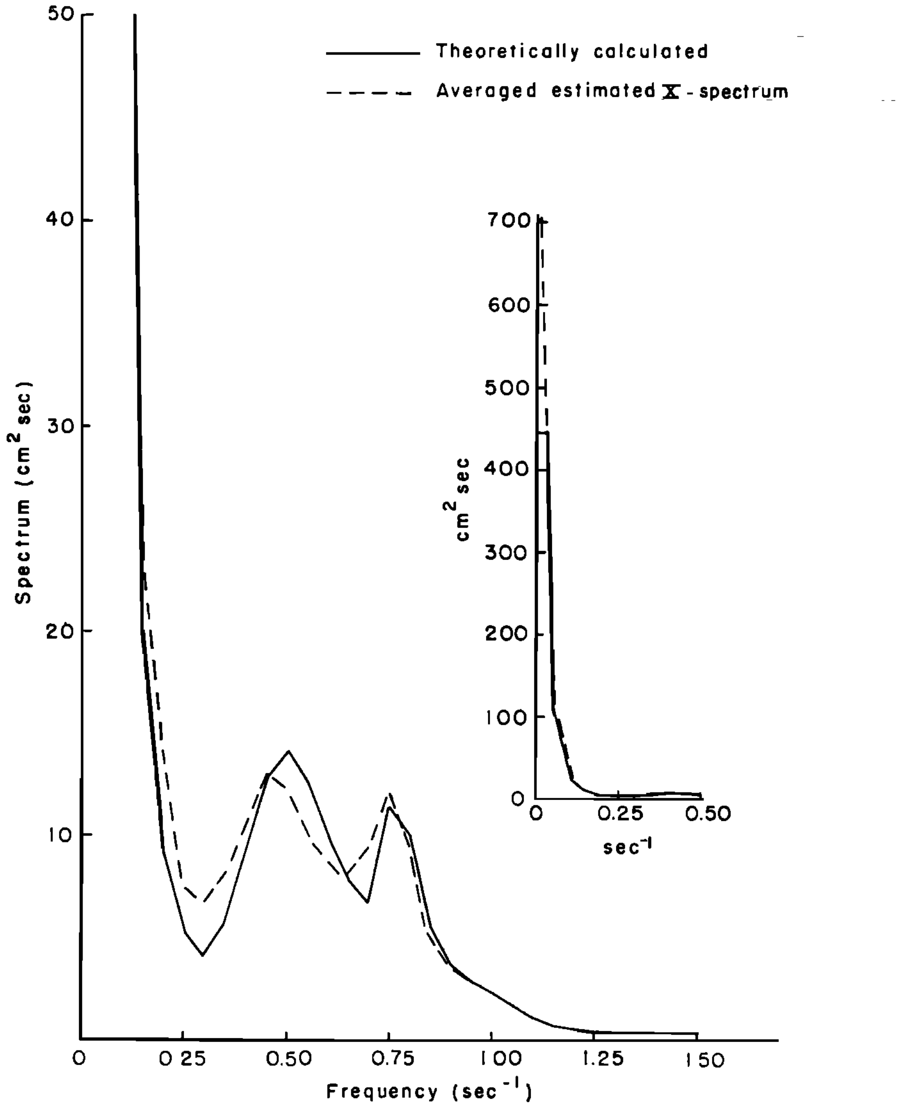

Fig. 7. The averaged estimated X spectrum obtained after removal of theoretical drift and the theoretical X spectrum.

An average X spectrum was calculated from the data after removing the theoretical drift instead of the observed drift for each run. Figure 7 shows both this average X spectrum and the theoretical X spectrum evaluated from the surface spectrum. The good agreement between these two curves shows that the low-frequency parts of the X spectrum can be better estimated by removing the theoretical drift and leaving a residual linear trend associated with each sample. The agreement between observation and theory would be better for continuous sample runs about ten times longer than those actually used in this experiment because the linear trend would then better approximate the drift and the oscillations about this drift would be removed correctly.

Estimate of the bispectrum. The bispectra of the horizontal and vertical motions of the sphere were estimated by Paul Shaman. Figure 8 is the amplitude of the corresponding bispectrum of Figure 3. The high values for the X

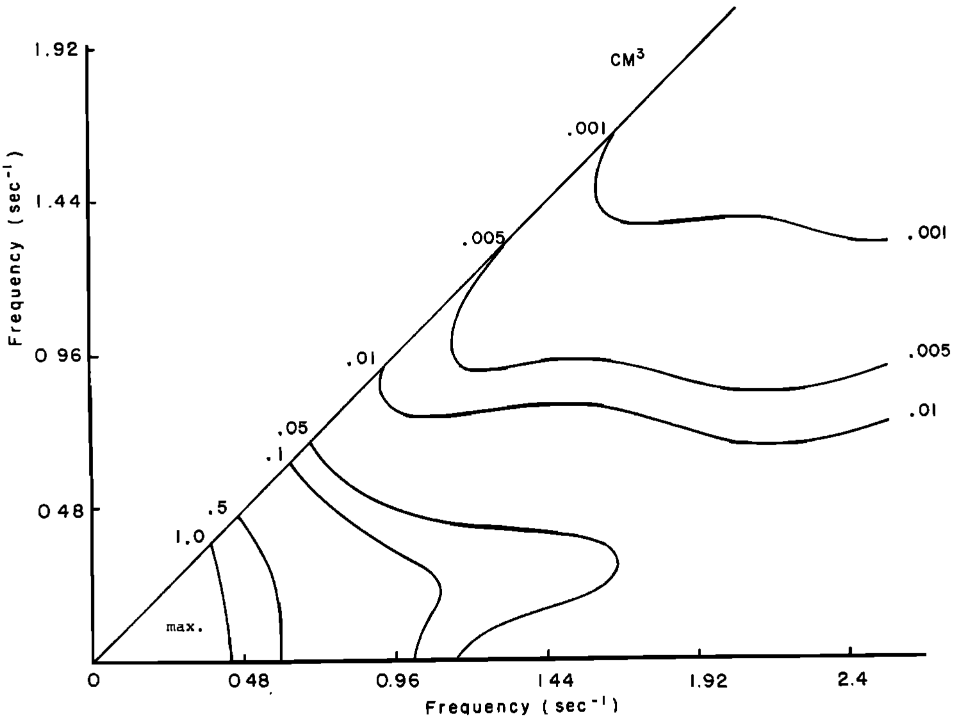

Fig. 8*a*. Amplitude of X bispectrum of Figure 3.

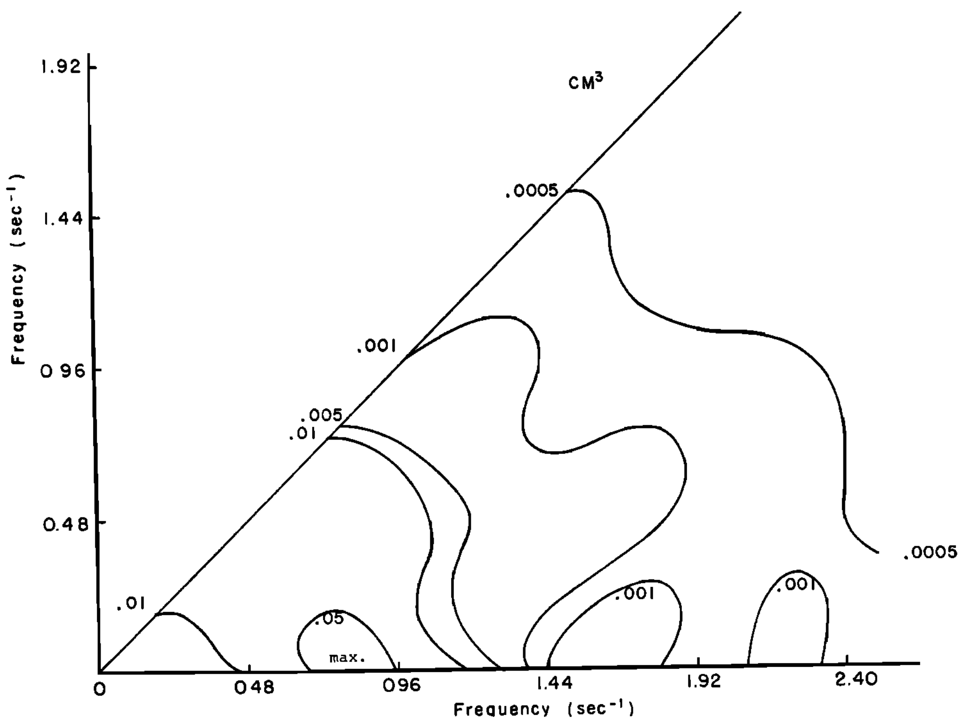

Fig. 8*b*. Amplitude of Z bispectrum of Figure 3.

bispectrum over the low-frequency area of the $\omega\omega'$ plane and the diagonal decrease of the bispectrum are expected from the theory as described previously. The estimated Z bispectra are quite small. Theoretically, the Z bispectrum should be approximately equal to zero, as discussed above. Therefore, the estimated bispectra are just what one would expect.

Conclusions

This study indicates the need of the second-order solution in describing the motion of particles in random gravity waves and demonstrates that the second-order solution approximates the motion of the particle very well.

To the first-order approximation, the spectra of the vertical and horizontal movements and their quadrature spectrum are identical. The high values over the low-frequency band of the experimental X spectrum and quadrature spectrum of X and Z (as shown in Figure 4) are missed in this model. To the second order, the irrotational model (equation 69) gives the right spectral corrections. The estimated bispectrum in the horizontal motion of the particle also shows this significant nonlinear effect.

From the first-order solution, it is suggested that no mean motion should appear in both the X and the Z coordinates. The experimental data show, however, a visible drift in the horizontal coordinate. This discrepancy has been removed by the second-order approximation. The mean velocity calculated from (73) is in substantial agreement with the experimental results (Table 1).

Acknowledgments. I wish to thank Professor Willard J. Pierson, Jr., for suggesting the topic and for his guidance and encouragement throughout the course of this research. I also wish to thank Dr. Leo J. Tick for his critical review of the manuscript, Professor A. D. Kirwan for his suggestions and advice, and Dr. Paul Shaman for the computations of the bispectra. Finally, thanks are due Mr. Vincent Cardone and the members of the Pacific Hindcasting Project for their help.

The research performed for the preparation of this paper was sponsored by the U. S. Naval Oceanographic Office, under contract N62306-1589, task order 3. More extensive graphs of the results are given in *Chang* [1968].

The research described in this paper has had a long history of support that needs to be acknowledged. The early work on studying waves in terms of the Lagrangian equations was supported by the Office of Naval Research and resulted in a report by *Pierson* [1961]. Funds to make the measurements described herein were provided by the National Science Foundation under grant G21970 and a preliminary analysis of the data was made, but not published, in 1963. The preparation of a motion picture describing the experiment was supported by the Office of Naval Research [*Pierson,* 1963].

References

Bagnold, R. A., Sand movements by waves: Some small-scale experiments with sand of very low density, *J. Inst. Civil Engrs., 27,* 447–469, 1947.

Beach Erosion Board, *Tech. Rept. 1,* U. S. Government Printing Office, Washington, D. C., 1941.

Chang, M.-S., The mass transport in deep water long crested random gravity waves, *Geophys. Sci. Lab. TR-68-1,* Department of Meteorology and Oceanography, New York University, 1968.

Corrsin, S., Theories of turbulent dispersion, Preprint, International Colloquium on Turbulence, University d'Aix-Marseille, August 28 to September 2, 1961.

de Caligny, A. F. H., Experiment sur les mouvements des molecules liquides des ondes courantes, considérés dans leur d'action sur la marche des navires, *Compt. Rend., 87,* 1019–1024, 1878.

Isserlis, L., On a formula for the product-movement coefficient of any order of a normal frequency-distribution in any number of variables, *Biometrika, 12,* 1918.

Kinsman, B., *Wind Waves; Their Generation and Propagation on the Ocean Surface,* Prentice-Hall, Englewood Cliffs, N. J., 1965.

Longuet-Higgins, M. S., Mass transport in water waves. *Phil. Trans. Roy. Soc. London, A, 245,* 535–581, 1953.

Longuet-Higgins, M. S., Mass transport in the boundary layer at a free oscillating surface, *J. Fluid Mech., 8,* 565–583, 1960.

Pierson, W. J., Models of random seas based on the Lagrangian equations of motion, *Tech. Rept. Contr. Nonr-285(03),* College of Engineering, Research Division, New York University, 1961.

Pierson, W. J., Perturbation analysis of the Navier-Stokes equation in Lagrangian form with selected linear solutions, *J. Geophys. Res., 67*(8), 3151–3160, 1962.

Pierson, W. J., Observations of long-crested random-breaking waves in both Lagrangian and Eulerian form for comparison with available theories, in *Time Series,* pp. 140–143, John Wiley. New York, 1963.

Stokes, G. G., On the theory of oscillatory waves, *Trans. Conf. Phil. Soc. Cambridge, 8,* 441–455, 1847.

Tick, L. J., A nonlinear random model of gravity waves, *J. Math. Mech., 8,* 643–652, 1959.

(Received July 9, 1968;
revised November 1, 1968.)